

Facile Nonpolar Organic Solution-Process to Nanostructure Hematite Photoanode with High Efficiency and Stability for Water Splitting

Jian-Jun Wang,^{1,*} Yelin Hu,^{1,2} Rita Toth,¹ Giuseppino Fortunato,³ Artur Braun^{1,*}

¹ Laboratory for High Performance Ceramics, Empa, Swiss Federal Laboratories for Materials Science and Technology, Ueberlandstrasse 129, CH-8600, Dübendorf, Switzerland. ² Laboratory of Photonics and Interfaces, Institute of Chemical Sciences and Engineering, Swiss Federal Institute of Technology, CH-1015 Lausanne, Switzerland. ³ Laboratory for Protection and Physiology, Empa, Swiss Federal Laboratories for Materials Science and Technology, Lerchenfeldstr. 5, CH-9000, St. Gallen, Switzerland.

E-mail: *wangjj@iccas.ac.cn and *Artur.Braun@alumni.ethz.ch

Experimental Section

Fabrication of hematite photoanode. 0.25 mmol Fe-oleate and 0.0075 mmol Tin (II) 2-ethylhexanoate were dissolved in 0.5 ml toluene as stock solution. The precursor solution was spin-coated on precleaned FTO glass slide at 3000 rpm for 60 seconds. The coated substrates were then sintered in air at 550 °C for 20 min after each layer coated to convert it to hematite. The substrates with desired thickness were sintered in air at 550 °C for 6h. Then, the hematite slides were transferred to a tube furnace to sinter in Ar at 550 °C for 6h.

Scanning electron microscopy

The morphology of hematite film was characterized using a high resolution field emission scanning electron microscope (SEM) (Hitachi S-4800 microscopy).

X-ray photoelectron spectroscopy

Surface compositions were characterised by XPS measurements, performed on a PHI 5000 VersaProbe II instrument (USA) with a monochromatic AlK α X-ray source. Energy resolution of the spectrometer was set to 0.8 eV/step at a pass-energy of 187.85 eV for survey scans and 0.125 eV/step and 29.35 eV pass-energy for high resolution region scans, respectively. Carbon 1s at 284.5 eV was used as a calibration reference to correct for charge effects. Elemental compositions were determined using instrument dependent atom sensitivity factors. Data analysis was performed by use of CasaXP software (Casa Software Ltd, United Kingdom).

UV-vis spectroscopy

UV-vis spectra were carried out on a Cary 5000 UV-Vis-NIR spectrophotometer.

Photoelectrochemical measurement

Photocurrents of the hematite photoanodes were measured in a three-electrode configuration photoelectrochemical cell (so-called cappuccino cell of PEEK plastic) with 1M NaOH (pH~13.6) as electrolyte, Ag/AgCl/sat. KCl as reference, and a platinum sheet (0.5 cm \times 0.5 cm) as counter electrode. The potential is reported relative to the reversible hydrogen electrode potential (RHE). The hematite electrode was scanned at 50 mV/s between 0.7 and 1.8V vs RHE. The potential of the working electrode was controlled by a Voltalab80 PGZ 402 potentiostat. The film was illuminated through the electrolyte and a fused silica window with a 0.5 cm 2 aperture. The light source was a 1.5 AM solar simulator (HAL 302 Solar Simulator, 350–750 nm, Asahi Spectra, Japan). The photocurrent action spectra were obtained under light from a 300W Xe lamp with an integrated parabolic reflector (Ceramx PE 300 BUX) and the light passed through a monochromator (Bausch & Lomb, bandwidth 10 nm). EIS measurements were performed at a frequency range of 1 Hz–100 kHz at 1.23V vs RHE and the magnitude of the modulation signal was 10 mV. The EIS spectra were fitted to the electrical analogue under study by means of the ZViews software. The electrochemical capacitances derived from the electrochemical impedance were measured in dark at a frequency of 1000 Hz. All the measurements were performed at room temperature.

Gas chromatograph (GC) measurement

H $_2$ generation from a custom designed airtight plastic PEC cell was monitored by a GC-2014 Shimadzu gas chromatograph. TCD detector and Haysep D 10' column were used and the temperatures of the injector, column and detector were 40, 30

and 140 °C, respectively. The flow rate on the column was 24 mL/min. The gases were automatically injected every 30 minutes into the GC in parallel with the chronoamperometry experiment.

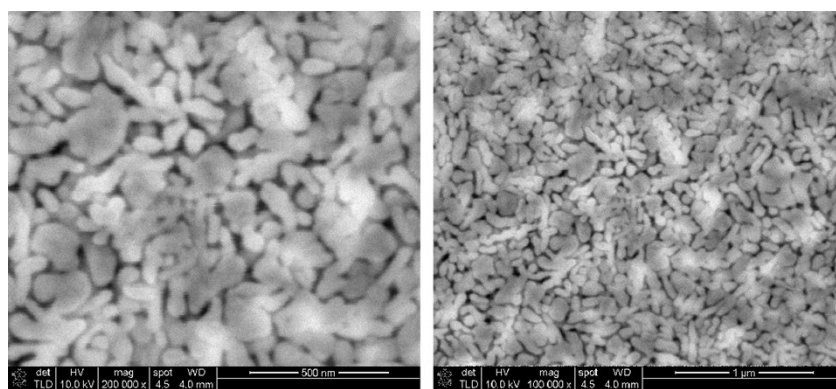


Figure S1. SEM images of undoped hematite film. The size bar in the left micrograph is 500 nm, the size bar in the right micrograph is 1 micrometer.

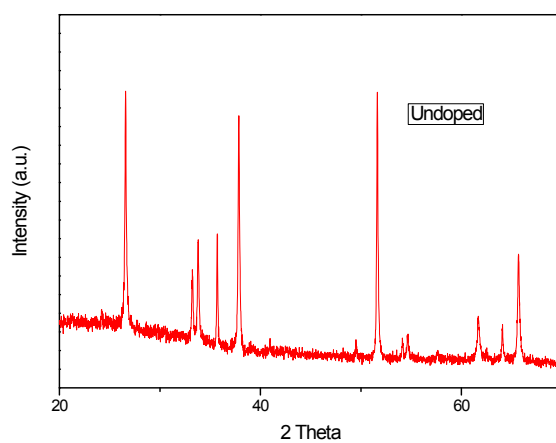


Figure S2. XRD pattern of undoped hematite film.

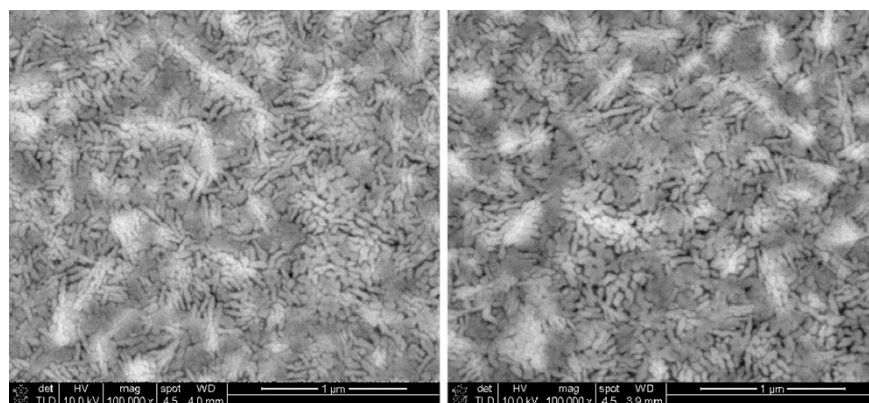


Figure S3. SEM images of doped hematite films before and after sintering in Ar.

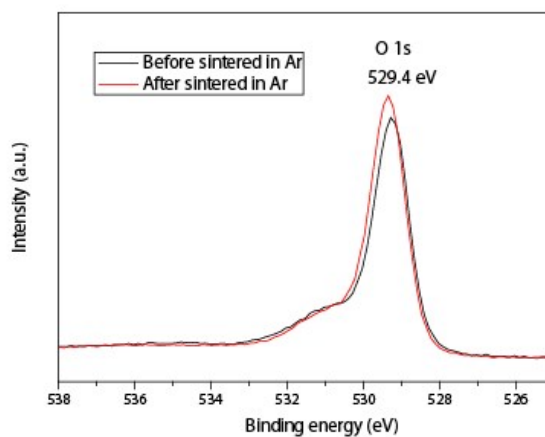
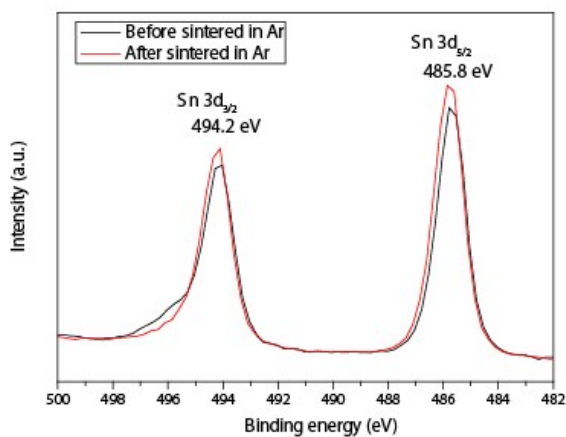
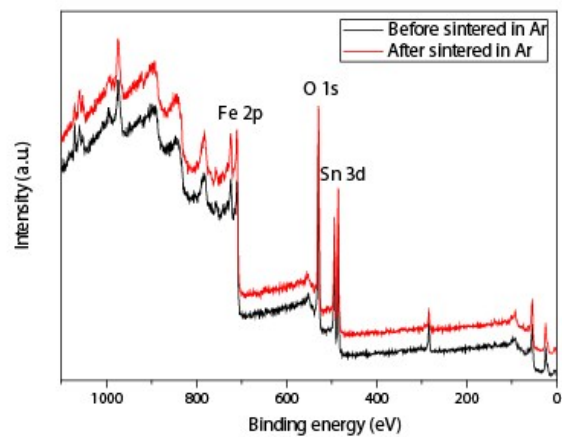


Figure S4. XPS spectra of doped hematite films before and after sintering in Ar. The shoulder peak of Sn 3d spectra is attributed to the FTO substrate since it was not observed in thicker samples. The shoulder peaks of O 1s, indicative of -OH is due to atmospheric exposure.

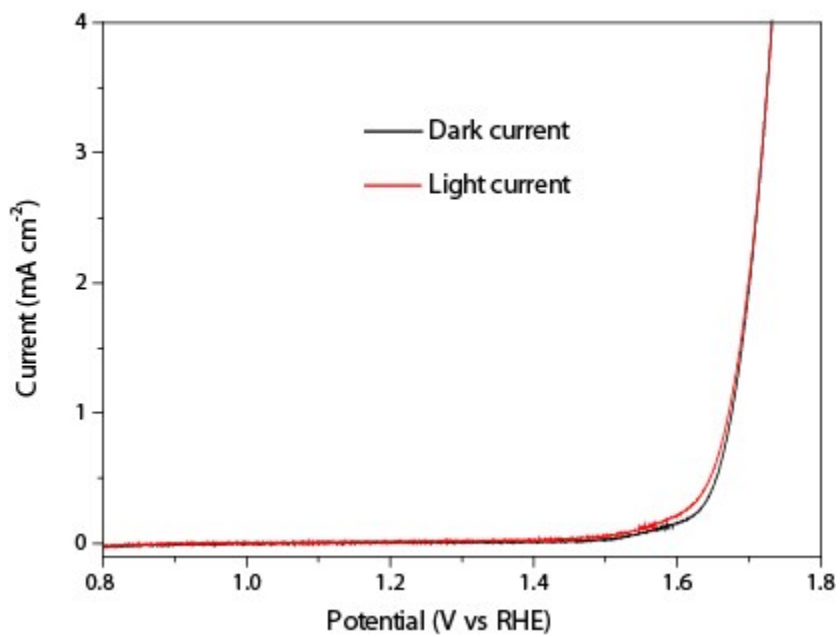


Figure S5. J-V curves of undoped hematite film.

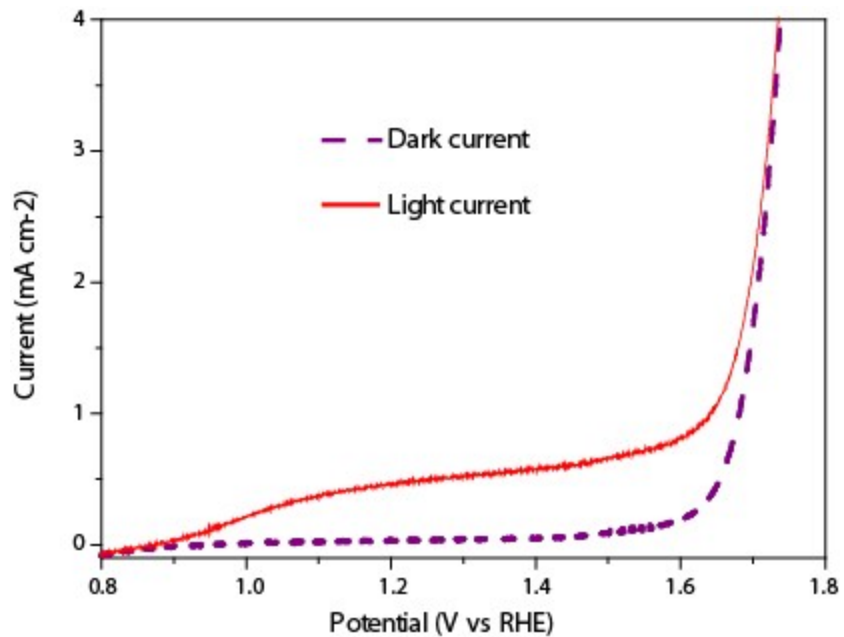


Figure S6. J-V curves of doped hematite photoanode sintered in Air for 12h.

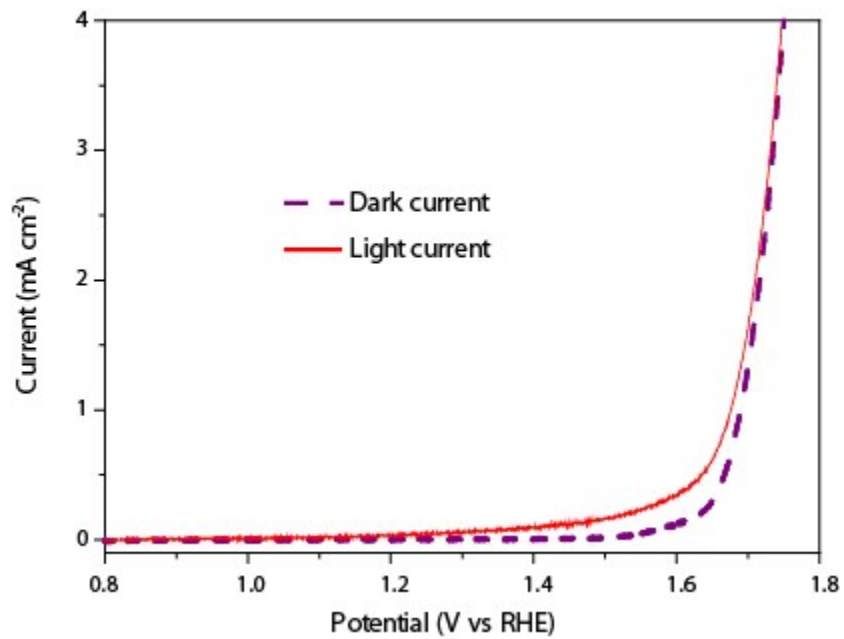


Figure S7. J-V curves of undoped hematite photoanode after sintering in Ar.

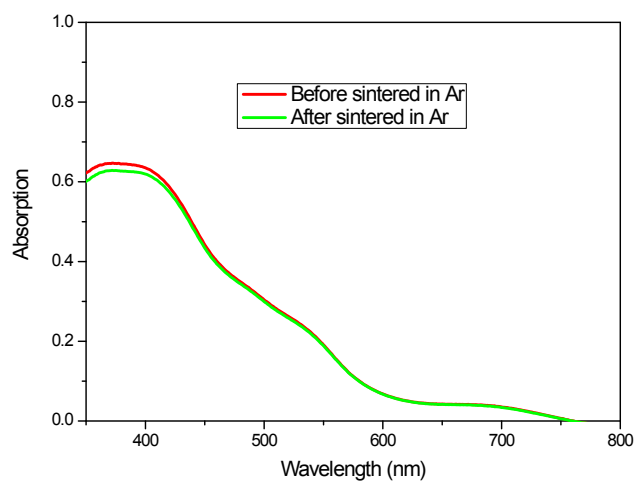


Figure S8. UV-vis spectra of doped hematite films before and after sintering in Ar.

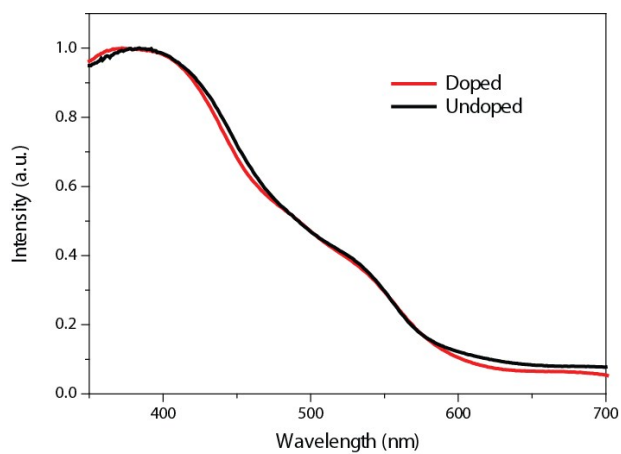


Figure S9. UV-vis spectra of doped and undoped hematite films.

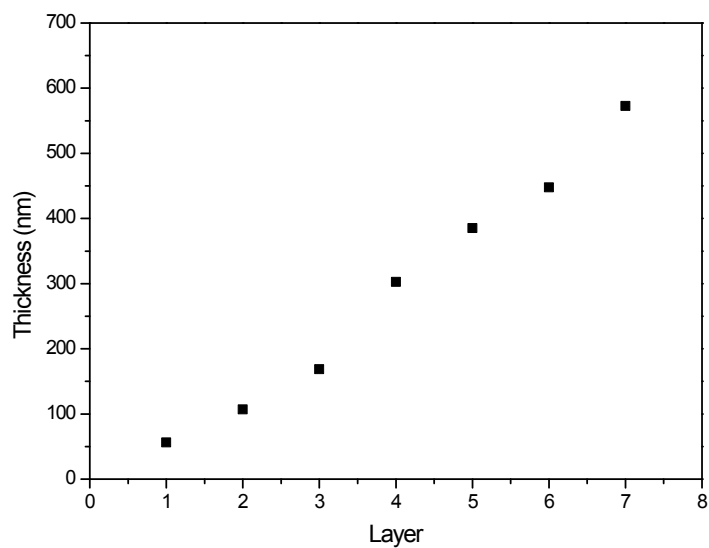


Figure S10. The relationship of layers and thickness.

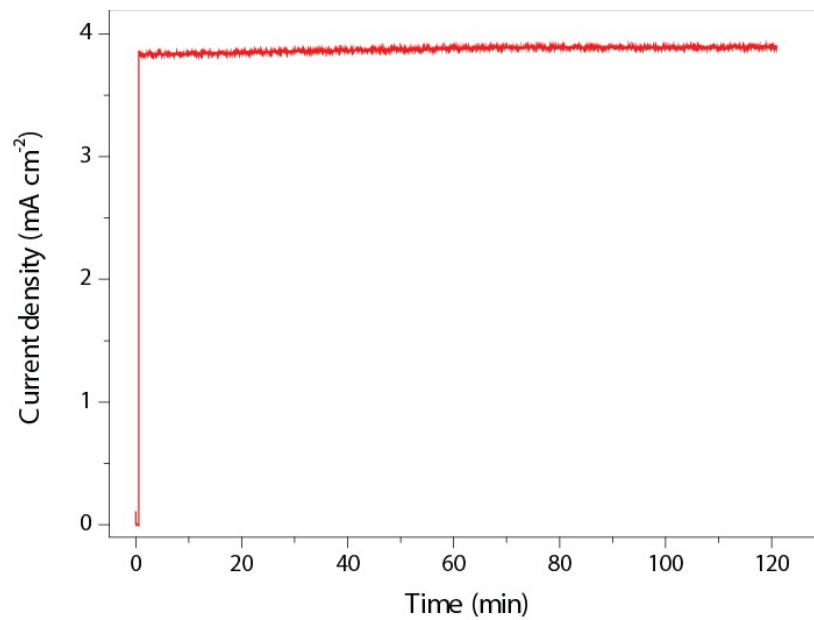


Figure S11. The stability of the sample with 5 layer thickness has been tested at 1.5 V vs RHE in light.

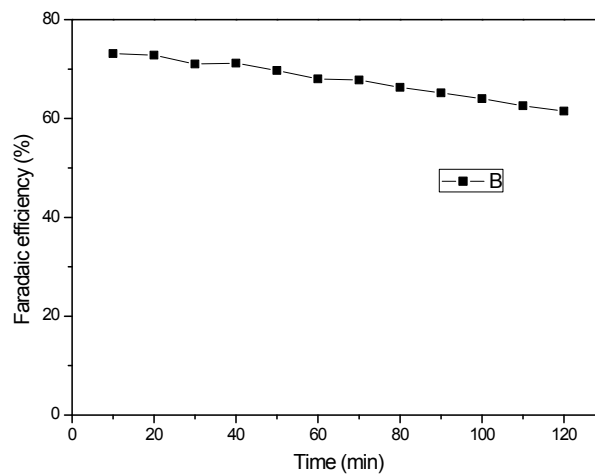
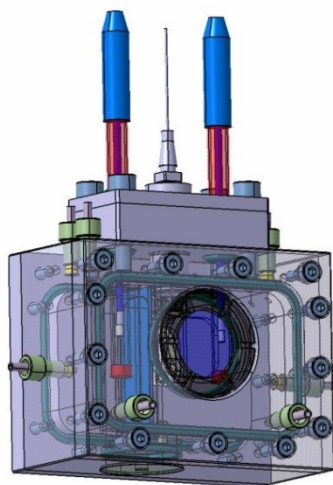


Figure S12. Sketch of PEC cell used for gas measurement and Faradaic efficiency of hydrogen generation. We believe the faradaic efficiency deviating from unity should be due to some systematic errors including gas leakage and gas loss in the solution.

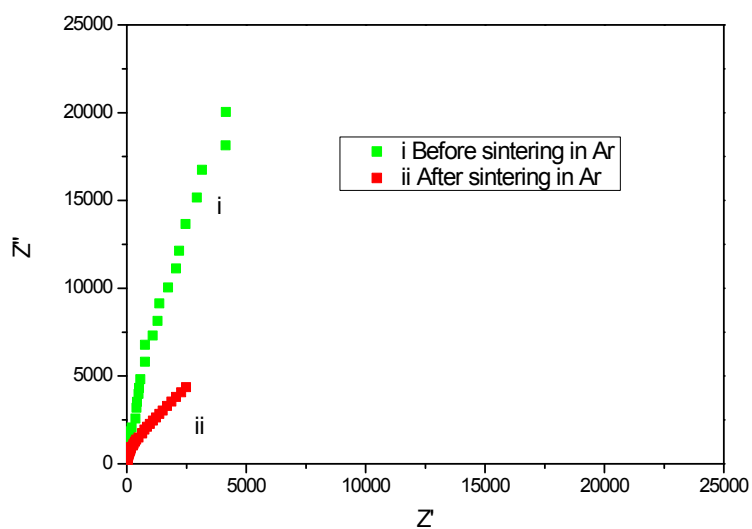


Figure 13S. Nyquist plots of doped hematite films before and after sintering in Ar measured at 1.23V vs. RHE in dark.

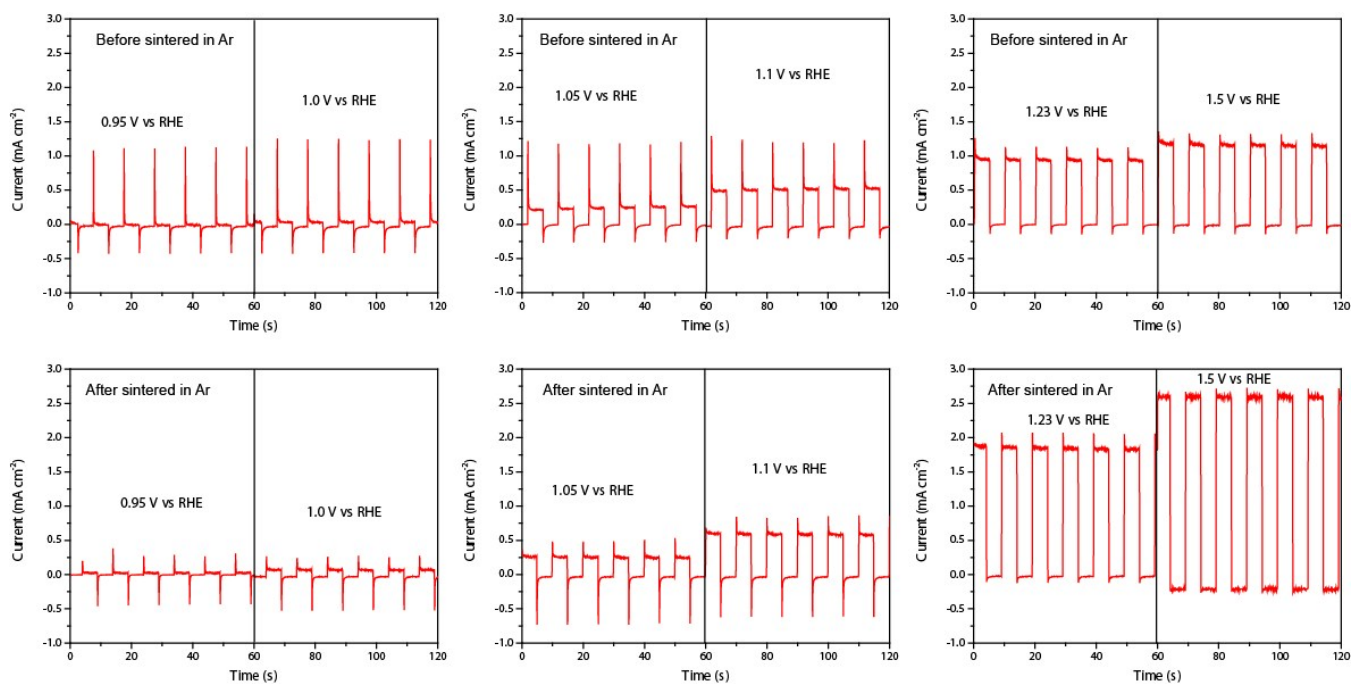


Figure S14. Transient current of doped hematite photoanode before and after sintered in Ar.